

## Structural and thermodynamic studies of KM+ , a D-mannose binding lectin from *Artocarpus integrifolia* seeds

Rosemeire A. Silva-Lucca<sup>a,b</sup>, Marcel Tabak<sup>b</sup>, Otaciro R. Nascimento<sup>a</sup>,  
Maria C. Roque-Barreira<sup>c</sup>, Leila M. Beltramini<sup>a,\*</sup>

<sup>a</sup>Instituto de Física de São Carlos, Universidade de São Paulo, Caixa Postal 369, São Carlos, SP, Brazil

<sup>b</sup>Instituto de Química de São Carlos, Universidade de São Paulo, Caixa Postal 780, São Carlos, SP, Brazil

<sup>c</sup>Faculdade de Medicina de Ribeirão Preto, Universidade de São Paulo, Ribeirão Preto, SP, Brazil

Received 21 September 1998; received in revised form 2 December 1998; accepted 5 March 1999

### Abstract

The KM+ lectin exhibits a novel and unusual circular dichroism (CD) spectrum that could be explained by a high proline content that would be inducing deformation of the  $\beta$ -structure and/or unusual turns. KM+ was shown to be a very rigid lectin, which was very stable under a broad variety of conditions (urea, guanidine, hydrolysis, pH, etc.). Only incubation for 60 min at 333–338 K and extreme basic pH were able to induce conformational changes which could be observed by CD and fluorescence measurements. Data from CD are typical for protein denaturing associated with changes in the overall secondary structure. Data from high-performance size exclusion chromatography (SEC) showed that the denatured forms produced at pH 12.0 are eluted in clusters that co-elute with the native forms. A significant contribution from the tyrosines to the fluorescence emission upon denaturation was observed above 328 K. In fact at 328 K some broadening of the emission spectrum takes place followed by the appearance of a shoulder (approx. 305 nm) at 333 K and above. The sensitivity of tryptophan fluorescence to the addition of sugar suggests a close proximity of the tryptophan residues to the sugar binding site,  $K_a = (2.9 \pm 0.6) \times 10^3 \text{ M}^{-1}$ . The fraction of chromophore accessible to the quencher obtained is  $f_a = 0.43 \pm 0.08$ , suggesting that approximately 50% of the tryptophan residues are not accessible to quenching by D-mannose. KM+ thermal denaturation was found to be irreversible and was analyzed using a two-state model (N  $\rightarrow$  D). The results obtained for the activation energy and transition temperature from the equilibrium CD studies were: activation energy,  $E_a = 134 \pm 11 \text{ kJ/mol}$  and transition temperature,  $T_m = 339 \pm 1 \text{ K}$ , and from the fluorescence data:  $E_a = 179 \pm 18 \text{ kJ/mol}$  and  $T_m = 337 \pm 1 \text{ K}$ . Kinetic studies gave the following values:  $E_a = 108 \pm 18 \text{ kJ/mol}$  and  $E_a = 167 \pm 12 \text{ kJ/mol}$  for CD and fluorescence data, respectively. © 1999 Elsevier Science B.V. All rights reserved.

**Keywords:** Lectin CD; Thermal denaturation; Chemical denaturation; Lectin fluorescence; Lectins from *Artocarpus integrifolia*; Denaturing of lectins

\*Corresponding author. Instituto de Física de São Carlos, Universidade de São Paulo, av. Dr Carlos Botelho, 1465, C.E.P. 13560-250, São Carlos, SP, Brazil. Fax: +55-16-2715381; e-mail: leila@ifsc.usp.br

## 1. Introduction

In recent years a strong stimulus for the study of lectins, a very diverse class of proteins, has appeared as a result of their ability to bind monosaccharides and oligosaccharides with high affinity and specificity. They are present in an extensive range of organisms (from viruses and plants to humans) and are able to mediate several biological events such as the recognition of molecules present in membranes or in the extracellular matrix. The lectins have been classified into families, according to their monosaccharide binding specificity. This property has found widespread application in probing the architecture and dynamics of cell surface carbohydrates during cell division, differentiation and malignancies as well as in the isolation and characterization of glycoconjugates [1–3]. As an example, in higher organisms members of the galectin family serve as receptors for  $\beta$ -galactoses and have a role in modulating cell–cell and cell–matrix interactions [4,5]. Due to their specificity and selectivity in the binding of carbohydrates, lectins have been used as tools in several studies of molecular mechanisms in biological systems [2]. On the other hand detailed studies of their properties and molecular structures have been of intensive interest in the design of carbohydrate-based therapeutic inhibitors of lectin-mediated interactions [6,7].

Two lectins which show interesting biological properties, jacalin and KM+, have been isolated from the seeds of *Artocarpus integrifolia* [8–10]. Jacalin is an important biotechnological tool due to its unique ability to specifically recognize IgA from human serum and milk [9] and its interaction with specific regions of CD4 thereby causing an inhibition in HIV-infection in vitro [11]. KM+ lectin directly induces neutrophil migration ‘in vivo’ (into the peritoneal cavity or into the air pouch of rats) and ‘in vitro’ (human neutrophils), agglutination of human red blood cells and proliferation of Balb/c mouse spleen cells as described earlier [10]. Recently, it was observed that the carbohydrate recognition site is responsible for the binding of KM+ to connective tissue and vascular endothelium [12]. Based on SDS-PAGE (sodium dodecyl sulphate-polyacrylamide gel

electrophoresis) and isoelectric focusing data KM+ is composed of four monomers, held together by non-covalent bonds [10] and recently the complete primary structure of KM+ was obtained and a molecular weight of 64 kDa for the tetramer was established [13]. It is an acidic lectin possessing two tryptophan and seven tyrosine residues per monomer, and comprising 38% hydrophobic amino acids, 9.2% proline and 1.8% carbohydrate (w/w) [10]. Its biological activities were inhibited by monosaccharides  $\alpha$ -D-mannose,  $\alpha$ -D-glucose and  $\alpha$ -methyl mannoside [10]. Crystals of KM+ have been obtained which belong to the orthorhombic system with space group  $C222_1$  [14].

In the present studies we demonstrate KM+ to be a very rigid lectin, presenting an unusual circular dichroism spectrum and secondary structure, and describe its stability under elevated temperatures, in the presence of chaotropic agents and at high values of pH. We also report the association constant for sugar binding, thermodynamic and kinetic parameters ( $E_a$ , activation energy and  $T_m$ , transition temperature), and the native and denatured forms isolated by molecular filtration, on high-performance liquid chromatography (HPLC) and monitored by circular dichroism (CD) and steady-state fluorescence.

## 2. Material and methods

### 2.1. Large scale purification, characterization and biological activity of lectin KM+

A crude extract of *Artocarpus integrifolia* seeds was prepared as described earlier [10] but scaled up 10 times. Characterization of KM+ (obtained after affinity chromatography on the Sepharose D-mannose column) and fKM+ (obtained after molecular filtration of KM+ on the Superdex 75 Hiload 16/60 column) was made by SDS-PAGE and amino acid analysis as described in Santos-Oliveira et al. [10]. The affinity chromatography on Sepharose D-galactose and Sepharose D-mannose proved to be an efficient procedure for preparative scale purification of KM+ and gel filtration on Superdex 75 HL 16/60 (fKM+) was useful for checking the molecular weight. The

yield was similar to that previously reported, approximately 2% of the total protein of the crude extract. The amino acid composition and electrophoretic data of the fractions denoted KM+ and fKM+ were very similar to those previously described [10]. Protein concentration was determined by amino acid analysis.

Biological activity was monitored by agglutination of human red blood cells of group AB or O (100  $\mu$ l, 2% in PBS, phosphate buffered saline) by incubation with 100  $\mu$ l of KM+ and fKM+ (250  $\mu$ g protein) for 30 min at 295 K. Agglutination, visible to the naked eye, was taken as a positive assay. The biological activity after purification, both before and after spectroscopic assay was monitored by the haemagglutination assay, demonstrating the native state of the protein.

## 2.2. High-performance size exclusion chromatography (SEC) of KM+

Samples of KM+ were prepared in PBS (pH 7.4) at 0.2 mg/ml concentration and in 20 mM acetate/borate/phosphate buffer (pH 9.0 and 12.0) at 0.25 mg/ml. Samples were incubated at 310 K for 60 min. The pH was adjusted by addition of HCl (1.0 M) or NaOH (2.0 M). Subsequently the samples were filtered by SEC on the Superdex 75 HR 10/30 column (Pharmacia LKB Biotechnology, Uppsala, Sweden) using HPLC (Bio-Rad, 2800), and eluted with the same incubation buffers containing 0.1 M of D-galactose and 0.1 M of D-mannose at 293 K, at a flow rate of 0.5 ml/min, monitored by absorbance at 280 nm, and collected in 0.5 ml fractions. On filtration at pH 12.0, two fractions were obtained and denoted pool 1 (eluted approx. 10 ml) and pool 2 (eluted approx. 20 ml). These fractions were reapplied to the same column under identical conditions. Standard sample proteins (BSA, chymotrypsinogen and cytochrome C) were used for column calibration.

## 2.3. Circular dichroism (CD) measurements

CD spectra were recorded using a Jasco J-720 spectropolarimeter over a wavelength range of 190–260 nm, under constant N<sub>2</sub> purging according

to the manufacturers instructions (Jasco). Measurements were made on KM+ and fKM+ samples at a protein concentration in the range of 0.12–0.18 mg/ml, in quartz cuvettes of 1 mm path length. Spectra were typically recorded as an average of eight scans. CD spectra of native KM+ were measured in PBS pH 7.4 or deionized water. The CD spectrum of KM+ in water which is given in Fig. 1 was recorded from 250 to 185 nm in order to demonstrate a more complete spectral range while in saline solution extensive noise is observed below 195 nm. Spectra were measured in PBS in order to best reproduce physiological conditions. The spectra of the fractions KM+ and fKM+ were very similar, so all subsequent spectroscopic measurements were made with the KM+ fraction. The stability of KM+ was studied as a function of temperature (298–353 K) and the following denaturing agents: sodium dodecyl sulphate (SDS, 1–52 mM), guanidine hydrochloride (GdnHCl, 0.1–6.0 M), and urea (1–6 M). The CD spectra of the fractions obtained by SEC were recorded in the same conditions. CD spectra were obtained on a degree ellipticity ( $\theta$ ) scale. They were transformed using the mean weight residue and concentration prior to the secondary structure analysis. The samples were incubated for 5, 10, 15, 30, 60, 240 min and 24 h in the range from 298 to 348 K, at 5 degree intervals followed by a rapid cooling to 298 K. In the case of equilibrium experiments the above samples were maintained for a fixed time (60 min) at a given temperature, followed by cooling to 298 K and subsequent measurement. In the case of kinetic studies, measurements were carried out after an incubation at a given temperature for a varied length of time. Aliquots of SDS, GdnHCl and urea were added to a separate single sample of KM+ in water for each concentration of denaturant and incubated at 298 K for 15, 60, 120 min and 24 h, before each measurement. CD spectra were recorded at various pH values in the range 2.2–12.0. Samples were dissolved in the following buffers (all of them containing 150 mM of NaCl): 10 mM glycine (pH 2.2–4.0), 10 mM ammonium acetate (pH 4.0–6.0), 10 mM PBS (pH 6.5–7.5), 10 mM Tris-HCl (pH 7.0–9.0), 10 mM 3-[cyclohexylamino]-1-propanesulphonic acid, CAPS (pH

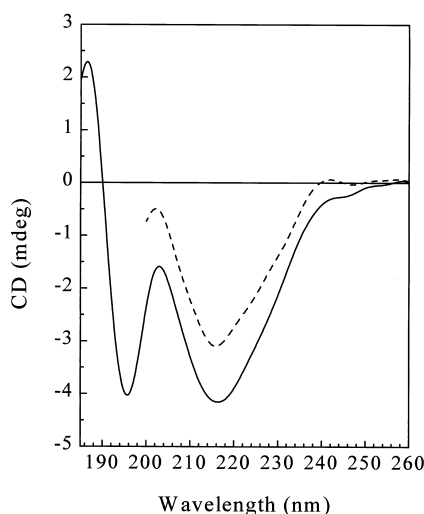


Fig. 1. CD spectra of KM+ (120–150  $\mu\text{g/ml}$ ) lectin at 298 K. The solid line represents the CD spectrum of KM+ in water and the dashed line shows the spectrum of KM+ in PBS buffer (pH 7.4).

9.0–10.5). Acetate/borate/phosphate/acetic acid, 20 mM, was also used as a buffer in the following manner: an aliquot of KM+ (at 4.0 mg/ml) was added to 4.5 ml of buffer and the pH was adjusted by addition of HCl (1.0 M) or NaOH (2.0 M), in the range 7.0–4.0 and 7.0–12.0, respectively.

#### 2.4. Estimation of secondary structure

Analysis of the CD spectra in terms of secondary structure content was performed using the Convex Constraint Analysis (CCA), developed by Perczel and Fasman, and based on the simplex algorithm. This method allows the deduction of the spectral contribution of the common secondary structures (deconvolution) through the direct use of the experimental CD curves of proteins [15,16].

#### 2.5. Fluorescence measurements

Fluorescence measurements were performed at 298 K on a Jasco FP-777 spectrofluorometer. Samples were excited at 280 and/or 295 nm and the emission was monitored in the range 290–450

nm and/or 300–455 nm. Quartz cuvettes (1 cm path length) of 1.0 or 3.0 ml volume were used for all the measurements. The protein concentration used in these experiments was in the range 0.09–0.12 mg/ml so that the optical density at 280 nm was always less than 0.1. Fluorescence measurements of KM+ were performed at varied pH and temperature and in the presence of varied concentrations of denaturants and quenchers. The buffers for pH experiments were the same as described for CD. Experiments with denaturants and quenchers were performed in PBS buffer. The protein fractions obtained by SEC, at pH 7.4, 9.0 and 12.0, were used for measurements in the same conditions. Measurements at varied temperature were made in water. The procedures for sample preparation for equilibrium and kinetic experiments were analogous to those for the CD measurements, except that samples were incubated in the range 298–348 K at temperature intervals  $< 5$  K. The denaturants, SDS (1–52 mM), urea (1–6 M) and GdnHCl (0.1–3.5 M), in PBS pH 7.4 were incubated with the protein for 15 min at room temperature (298 K) prior to measurement. Fluorescence quenching was studied with 6.0 M stock solutions of KI, containing 0.1 mM  $\text{Na}_2\text{S}_2\text{O}_3$  to prevent formation of  $\text{I}_3^-$ . Titrations were performed by addition of small aliquots to the sample solution of 3-ml volume directly in the cuvette. To estimate the number of carbohydrate binding sites, a protein solution of fixed concentration (12  $\mu\text{M}$ ) was titrated directly in the fluorescence cuvette with a stock solution of D-mannose in PBS, pH 7.4 by addition of small aliquots resulting in a concentration variation in the range 0–240  $\mu\text{M}$ . After the addition of each aliquot of D-mannose an incubation time of 15 min was allowed at 298 K before measurement.

#### 2.6. Analysis of thermal denaturation

The ellipticity and fluorescence data obtained from the study of thermal denaturation of KM+ were analyzed assuming that this is an irreversible two state process [17]

$$\text{N} \xrightarrow{k} \text{D} \quad (1)$$

where N and D represent the native and irreversibly denatured forms of the protein, respectively, and  $k$  is a first order rate constant which changes with temperature according to the Arrhenius equation,

$$k = A \exp(-E_a/RT) \quad (2)$$

The fraction of denatured protein,  $f_d$ , is calculated from the relationship

$$f_d = (S_n - S_{\text{obs}})/(S_n - S_d) \quad \text{and} \quad f_n + f_d = 1 \quad (3)$$

in which  $S_{\text{obs}}$  is the ellipticity (in the case of CD) or the total fluorescence obtained from the area of the emission spectra (in the case of fluorescence) of the sample at a particular temperature;  $S_d$  and  $S_n$  are the values of  $\theta$  or of the area of the emission spectra, characteristic of the denatured and native states. The transition curve  $f_n$  can be expressed as a function of the temperature,  $T$ , according to [18]:

$$\ln[\ln(1/f_n)] = (E_a/R)(1/T_m - 1/T) \quad (4)$$

Thus, Eq. (4) can be used to estimate the activation energy of the reaction,  $E_a$ , and the temperature of transition,  $T_m$ .

Similarly, kinetic data obtained at a constant temperature were treated according to the simple first-order reaction (Eq. 1). Rate constants,  $k$ , were determined by using the usual semi-logarithmic plot:

$$\ln(f_n) = \ln[(S_t - S_f)/(S_0 - S_f)] = -kt \quad (5)$$

where  $S_t$  is the ellipticity or the total fluorescence (area of the emission spectra), at time  $t$ ,  $S_f$  stands for the corresponding value at very long times, and  $S_0$  represents the signal of native KM+. These values of  $k$  were used to construct the Arrhenius plot ( $\ln k$  vs.  $1/T$ ), and from this plot the activation energy was calculated.

The CCA algorithm was used to deconvolute the fluorescence spectra, obtained as a function of temperature, into two and three components [19]. These deconvolutions were made to check two alternative transition state models: two state

$N \rightarrow D$  or three state  $N \rightarrow I \rightarrow D$ . In these calculations we used the emission spectra at several temperatures (from 298 to 348 K) obtained for a fixed incubation time of 60 min. The fractions of denatured lectin,  $f_d$ , were calculated from the relationships:

$$y(x) = f_n N + f_d D \quad (6a)$$

$$y(x) = f_n N + f_d D + f_i I \quad (6b)$$

where  $y(x)$  refers to a given experimental fluorescence spectrum, N, D and I are the component emission spectra for the native, denatured and intermediate states;  $f$ 's are the fractions of each state. The emission spectra obtained from this deconvolution were also used to analyse the fluorescence spectra at a fixed temperature and for different incubation times, yielding Arrhenius plots.

### 3. Results

#### 3.1. CD spectroscopy and estimated secondary structure content

The CD spectrum of KM+ , in water, was characterized by two minima near 196 and 216 nm, two maxima near 203 and 188 nm, and a negative to positive crossover at 192 nm (Fig. 1). The spectra of the fractions KM+ and fKM+ were very similar, so all spectroscopic measurements were made with KM+. The CD spectrum of KM+ in PBS has intensive noise below 200 nm, so the spectrum of KM+ in water was used for secondary structure estimation. Both spectra in Fig. 1 have a very similar shape, the shift of the two curves being due to the different concentrations used. The shape of this spectrum is characteristic of KM+ and its low amplitude is consistent with KM+ being a non-helical protein. The secondary structure content was estimated using the CCA program and the following results for the fractions obtained:  $\alpha$ -helix 1.0%, parallel  $\beta$ -sheet and/or  $\beta$ -turn 21%, antiparallel  $\beta$ -sheet 15%, unordered form 28%, additional contributions (aromatic residues and disulphide bridges) 35% and an RMS (root-mean-square) of 1.0%

[15,16]. Similar results were obtained with the fraction  $f_{KM+}$ .

### 3.2. Conformational stability of $KM+$ as a function of temperature equilibrium studies

In order to show that the observed denaturation is a two step process we followed the CD spectral changes for 24 h at all temperatures. After 60 min it was observed that the CD spectra did not reach their final form corresponding to the denatured protein. In fact even after 4-h incubation the final form was not reached since the CD spectra of samples incubated for 60 and 240 min in the range from 298 to 348 K are identical. After 24 h incubation the CD spectra for samples exposed to 328 K or above are identical to the CD spectrum of the sample exposed to 348 K. This means that the denaturation as accompanied by CD spectral changes is indeed a slow process. In our calculations the spectra recorded after incubating the samples for up to 1 h were used, based on the fact that during this period the biological activity is maintained. Thus at temperatures up to 328 K, the slow spectral changes observed for longer incubation times refer to the denatured protein. In Fig. 2A the CD spectra of  $KM+$  as a function of temperature are presented. Below 328 K, for a 60 min period, the CD spectra remain essentially unchanged as compared to the spectrum at 298 K (native). Above 328 K, for a 60 min period, and in the wavelength range between 195 and 210 nm spectral changes in the CD spectra are quite pronounced, showing a considerable change near 203 nm. At 333 K, for a 60-min period, the haemagglutination assay showed that the protein was totally inactive. It is likely, therefore, that the CD spectra in the range 338–348 K correspond to a significantly unordered structure, consistent with the loss of the native secondary structure and biological activity that should accompany protein denaturing (at 353 K denatured  $KM+$  produces aggregates visible to the naked eye). In Fig. 2B the denatured fraction of  $KM+$ , as calculated from the ellipticity at 203 nm (Eq. 3), is shown. This curve suggests that there are no intermediates present in detectable amounts during the denaturation. The  $KM+$  de-

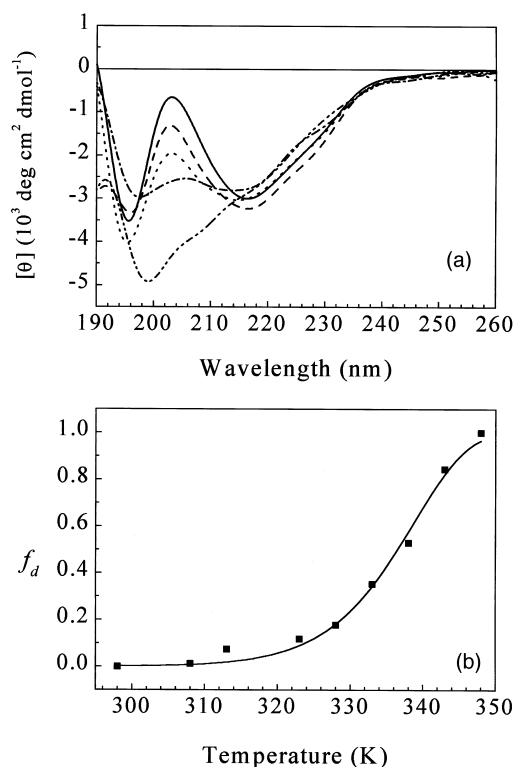


Fig. 2. CD spectra of  $KM+$ , in water, as a function of temperature. (A) Samples were incubated for 60 min and the spectra were recorded after incubation at 298 K (solid line), 328 K (dashed line), 333 K (dotted line), 338 K (dash-dot line) and 348 K (long-dashed line). (B) Thermal denaturing transition for the data from (A). The fraction of denatured protein ( $f_d$ ) was calculated as indicated in the text. The solid line represents the transition curve calculated according to an irreversible two state model [Eq. (4)]. The activation energy ( $E_a$ ) and the transition temperature  $T_m$  obtained from this fit are  $134 \pm 11$  kJ/mol and  $339 \pm 1$  K, respectively.

naturation was found to be irreversible, since samples that were heated above 328 K did not return to their original state even after rapid cooling back to 298 K or slow cooling to room temperature. Fig. 2B was analyzed by an irreversible two-state model [Eqs. (3) and (4)], and the solid line corresponds to the theoretical fit of the data. The parameters obtained were  $E_a = 134 \pm 11$  kJ/mol and  $T_m = 339 \pm 1$  K. The identical nature of the final spectra after 24 h incubation at 328 K or above compared to the spectrum of the sample incubated at 348 K favours our interpreta-

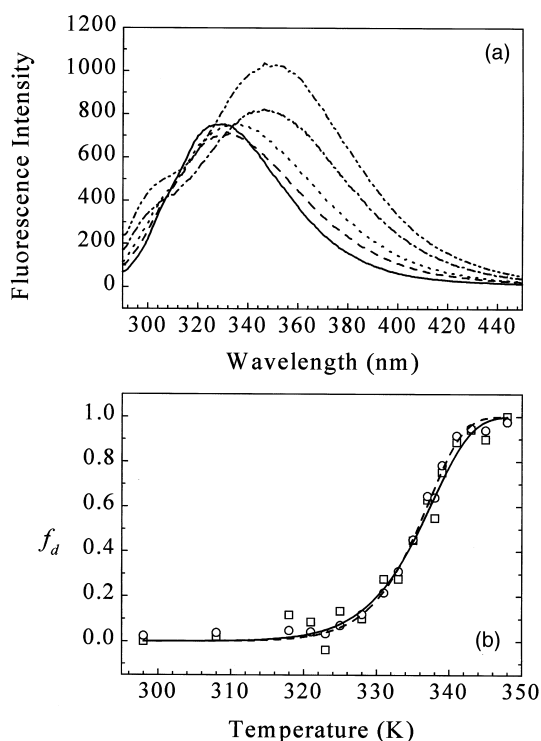


Fig. 3. Fluorescence emission spectra of KM+ in water, as a function of temperature. (A) Spectra after 60 min of incubation at temperatures of 298 K (solid line), 328 K (dashed line), 333 K (dotted line), 338 K (— · — · —) and 348 K (— · — · —). (B) Thermal denaturing transition for the data from (A): squares, calculated from the area of emission spectra and circles, calculated by the CCA algorithm. The lines represent the transition curves obtained according to an irreversible two state model [Eq. (4)]: solid, from area of the emission spectra data ( $E_a = 179 \pm 18$  kJ/mol and  $T_m = 337 \pm 1$  K), and dashed, from data obtained by CCA deconvolution ( $E_a = 206 \pm 18$  kJ and  $T_m = 337 \pm 1$  K).

tion of a two-state denaturation reaction.

Fluorescence of native KM+ was excited at 280 nm and emission spectra were monitored in the range of 290–450 nm. The emission maximum near 328 nm (Fig. 3A) is typical for tryptophan residues buried inside the protein [20,21]. The fluorescence quantum yield,  $\Phi$ , was measured as the total emission using tryptophan as a standard and the value of  $\Phi$  for KM+ in water is 0.045.

In Fig. 3A the fluorescence emission spectra as a function of temperature are presented. In the temperature range between 298 and 328 K the

fluorescence intensity presents a small decrease and the wavelength of maximum emission,  $\lambda_{\text{max}}^{\text{emis}}$ , is essentially constant at 328 nm. Above 328 K there is a pronounced red shift for the  $\lambda_{\text{max}}^{\text{emis}}$  together with an increase in intensity as well as an increase in the linewidth of the emission band. The value of  $\lambda_{\text{max}}^{\text{emis}}$  at the highest temperature (343–348 K) is 350 nm, which is quite typical for exposed tryptophan residues in proteins. Besides these changes the appearance of a shoulder around 305 nm is observed at the higher temperatures. The increase in the linewidth of the emission spectrum is due to the contribution from tyrosine residues, which have a characteristic emission maximum around 304 nm [22]. In general it is quite difficult to resolve the tyrosine emission in tryptophan containing proteins. By changing the excitation wavelength to 290 nm this shoulder can be made to disappear. Below 328 K the tyrosine emission is probably totally quenched either by nearby protein residues or due to energy transfer to the tryptophans [22]. The change in the denatured fraction was calculated for the data in Fig. 3A, using the total fluorescence (area of the emission spectra) as a parameter and this dependence is presented in Fig. 3B (squares). The full line represents the transition curve calculated according to Eq. (4). This plot is similar to the one described for CD data and suggests the existence of a two-state process. The activation energy and transition temperature obtained from the fit are  $179 \pm 18$  kJ/mol and  $337 \pm 1$  K, respectively.

The deconvolution of the fluorescence spectra using the CCA algorithm into three components (Eq. 6b) resulted in spectra very similar to those obtained using only two components. Therefore it can be concluded that two components are sufficient to describe the deconvolution of the whole set [15]. From these two component spectra the native ( $f_n$ ) and denatured ( $f_d$ ) fractions were calculated according to Eq. (6a). The plot of  $f_d$  vs.  $T$  is similar to those in Fig. 2B and Fig. 3B (squares), and the fit of the data according to Eq. (4) gave an  $E_a = 206 \pm 18$  kJ and a  $T_m = 337 \pm 1$  (Fig. 3B, circles). The choice of the total fluorescence (area of the emission spectra) or spectral decomposition (CCA) for determination of  $f_d$  is

due to the fact that these parameters seem to describe the overall process and are independent of a particular wavelength in the spectrum. We have also considered using the fluorescence intensity at 350 nm which yielded similar results to those in Fig. 3B. On the other hand, the fit using  $\lambda_{\text{max}}^{\text{emis}}$  to calculate  $f_d$  gave an activation energy for the process, which was more than 50% higher than that obtained with the parameters described above. It has been reported in the literature [23] that  $\lambda_{\text{max}}^{\text{emis}}$  is not a good parameter to monitor  $N \rightarrow D$  transitions and it has been suggested that fluorescence intensity, quantum yield (corresponding to total fluorescence) are better parameters to describe this process.

### 3.3. Kinetic studies

In Fig. 4 the variation of the ellipticity at a fixed temperature, expressed via the parameter  $f_n$ , corresponding to the fraction of native structure, is shown as a function of time for several temperatures. The data were fitted to a straight

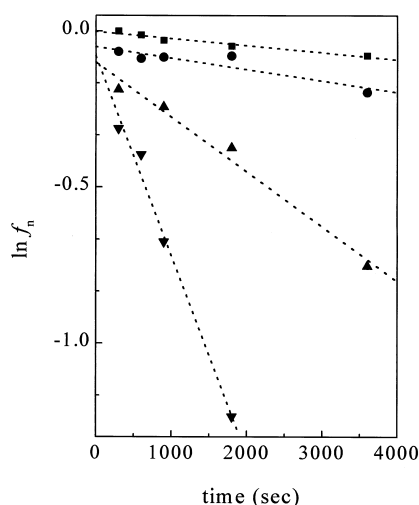


Fig. 4. Plot of kinetic studies for CD data. Plot of  $\ln f_n$  vs. time at the following temperatures: 298 K (squares), 328 K (circles), 333 K (up triangles), 338 K (down triangles).  $f_n$  is the native fraction of KM+, calculated as indicated in the text. The straight lines are linear regression fits, whose slopes yielded an estimate of the first order rate constant ( $k$ ). The slope of this Arrhenius plot gives the value of  $E_a = 108 \pm 18$  kJ/mol.

line on the semi-logarithmic plot and the rate constants  $k$  were obtained from the slopes [Eq. (5)]. From the Arrhenius plot for the data presented in Fig. 4 a value of  $108 \pm 18$  kJ/mol was obtained for  $E_a$ .

Similarly the variation of the area of fluorescence emission at a fixed temperature, expressed through the parameter  $f_n$ , was calculated as a function of time for several temperatures. The data were also fitted to a straight line on the semi-logarithmic scale and the rate constants ( $k$ ) were obtained from the slopes in the same way as for the CD data. The Arrhenius plot for these data also suggests the existence of a two state process and the  $E_a$  obtained was  $167 \pm 12$  kJ/mol.  $E_a$  from the slope of the Arrhenius plot using the data obtained from Eq. (6a) was  $161 \pm 12$  kJ/mol (CCA algorithm).

### 3.4. Structural changes of KM+ as a function of pH and chemical denaturants

Fluorescence and CD spectroscopy were used to monitor the structural changes of KM+ as a function of pH. In the fluorescence spectroscopy excitation at 280 nm of a solution of KM+ gave an emission spectrum in the range 290–450 nm with the emission maximum,  $\lambda_{\text{max}}^{\text{emis}}$ , near 328 nm at pH 7.0, which is for the emission from typical buried tryptophans inside proteins. Below pH 7.0 a small decrease in  $\Phi$  is observed suggesting a transition in the pH range 7.0–3.0; above pH 7.0 there is a pronounced decrease in the fluorescence emission intensity as shown in Fig. 5A. The wavelength for maximum emission is constant at 328 nm in the range from pH 2.2 to 9.5. Only at values of pH above 10.0 does the  $\lambda_{\text{max}}^{\text{emis}}$  change, reaching 340 nm at pH 12.0 (Fig. 5B). These changes in fluorescence emission following excitation at 280 nm also include contributions from tyrosine emission besides that from the tryptophan residues. This contribution is only apparent, above pH 10.5 and may be associated with a more global structural change to the monomers. The CD spectra were very similar for KM+ at pH between 2.2 and 11.5, raising the pH to 12.0, however, induced a large change in the spectrum (Fig. 6). This result strongly suggests that the



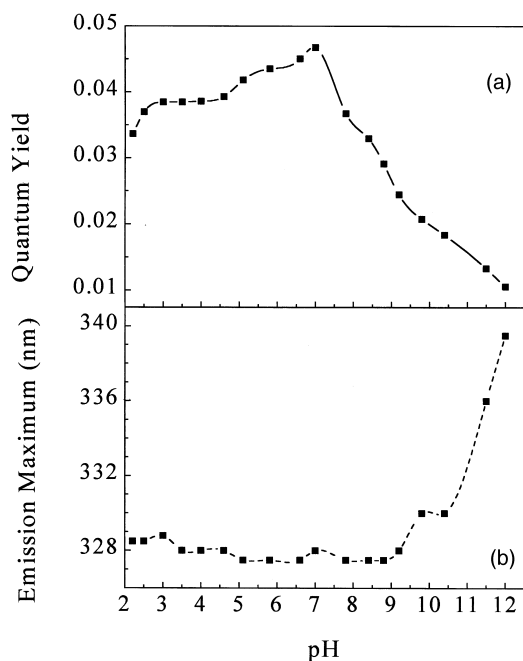


Fig. 5. The pH-dependence of fluorescence emission by  $KM^+$ . (A) Effect of pH on the quantum yield,  $\Phi$ . The buffers used were: glycine (pH 2.2–4.0) and acetate/borate/phosphate/acetic acid 20 mM (pH 4.0–12.0). (B) Wavelength of maximum emission of  $KM^+$  as a function of pH.

secondary structure of  $KM^+$  is not altered by acid or basic pH, except at extreme basic pH values. The changes in fluorescence are evident both as an increase in tryptophan residue exposure above pH 10.0 and as the quenching of fluorescence observed above pH 7.0. The results shown in Fig. 7 are from SEC of  $KM^+$  on the Superdex 75 column incubated and eluted at pH 9.0 (Fig. 7A) and pH 12.0 (Fig. 7B). The elution profile at pH 7.4 (native form) is identical to that observed at pH 9.0. The fraction which elutes at approximately 10 ml at pH 9.0 has the same CD and fluorescence spectra as native  $KM^+$  (tetrameric form). However, pool 1 from the pH 12.0 profile which eluted at the same position as the tetrameric form at pH 9.0 shows pronounced changes in the CD spectrum compared to both the pH 12.0 sample and the native protein (Fig. 6). The fluorescence quantum yield of pool 1 was 20% lower than that of the pH 12.0 sample. Pool

1 also showed a maximum fluorescence at a lower wavelength (336 nm) than the pH 12.0 sample (340 nm). These results showed that the denatured form of  $KM^+$  is eluted in aggregates that co-elute with the native form in SEC. Pool 2 from the pH 12.0 profile, eluted at approximately 20 ml (Fig. 7B) also shows an altered CD spectrum (Fig. 6) and its fluorescence spectrum shows the  $\lambda_{\text{max}}^{\text{emis}}$  to be shifted to 350 nm and  $\Phi$  to be reduced 60% compared with  $KM^+$  at pH 12. Pools 1 and 2 from SEC of  $KM^+$  at pH 12.0 were rechromatographed in the same conditions and the pool 1 reproduced the same profile as obtained in the Fig. 7B, while pool 2 showed only one fraction eluting in the original position (approx. 20 ml, figure not shown).

The results of addition of SDS, GdnHCl and urea to the solution of  $KM^+$  in PBS or water are totally consistent with a rigid structure since no significant changes were observed both in the tryptophan fluorescence and CD spectra. This is in good agreement with the fact that the only way to obtain the protein in monomeric form in SDS-PAGE experiments was to boil the protein solu-

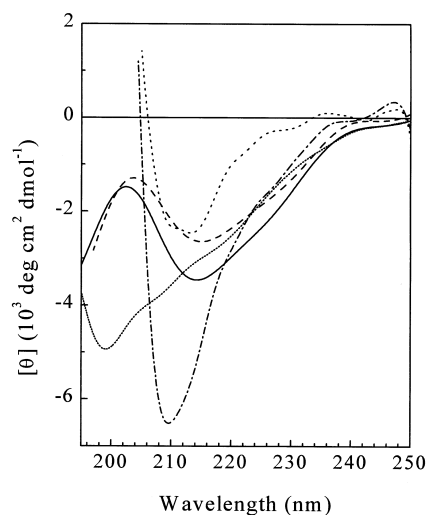


Fig. 6. CD spectra of  $KM^+$  as a function of pH. The samples were incubated in acetate/borate/phosphate/acetic acid, 20 mM, at 310 K, for 1 h. The spectra were recorded at the following pH values: 7.4 (solid line), 12.0 (dashed line), pool 1 from SEC pH 12.0 (— · — · —), pool 2 from SEC pH 12.0 (dotted line). The short dotted line shows the thermal denatured spectrum (348 K).

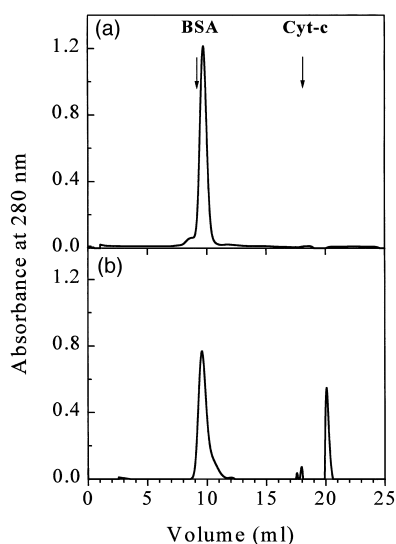


Fig. 7. High-performance size exclusion chromatography (SEC) of KM+ forms as a function of pH. The samples were incubated in acetate/borate/phosphate/acetic acid, 20 mM, at 310 K, for 1 h, at pH 9.0 (A) and 12.0 (B). The protein concentration was 0.25 mg/ml. The column, Superdex 75, 1 cm  $\times$  30 cm, was equilibrated with the buffer in the same pH as the sample, 0.5 ml/min and 293 K. D-mannose (0.1 M) and D-galactose (0.1 M) were included in the buffers and absorbance was monitored at 280 nm. The arrows indicate the elution positions of BSA and cytochrome C.

tion extensively. These results are also consistent with those from the thermal denaturation studies reported above, which show that up to approximately 333 K no significant changes are observed in either fluorescence emission or in the CD spectra.

### 3.5. Quenching of fluorescence of KM+

The intensity of KM+ fluorescence emission measured either after dissolving the lectin in PBS (pH 7.0, 7.2, 7.4) or in de-ionized water was essentially constant. In order to estimate the fluorescence quenching of KM+ as a function of D-mannose, KI and acrylamide, fluorescence titration of protein solutions was performed by addition of increasing concentrations of stock solutions of D-mannose, KI, and acrylamide into the fluorescence cuvette. The tryptophan residues of KM+ are not accessible to quenching either by

acrylamide or by iodide, for which a Stern–Volmer quenching constant ( $K_{SV}$ ) of  $0.9 \text{ M}^{-1}$  is obtained. In the case of D-mannose quenching, the data were fitted more appropriately through the use of the modified Stern–Volmer plot, namely the Lehrer plot [22], using  $A_0/\Delta A$  vs.  $1/[\text{mannose}]$ , where  $A_0$  and  $\Delta A = A_0 - A$  are the area of emission spectrum in the absence of the quencher and the difference of areas of emission spectra in the absence and presence of quencher (data not shown). From this plot an association constant,  $K_a$  of  $(2.9 \pm 0.6) \times 10^3 \text{ M}^{-1}$  was obtained for D-mannose. The fraction of chromophore accessible to the quencher ( $f_a$ ) obtained from this data is  $0.43 \pm 0.08$ , suggesting that approximately 50% of the tryptophan residues are not accessible to quenching by D-mannose. The sensitivity of tryptophan fluorescence to the addition of sugar suggests a close proximity of the tryptophan residues to the sugar binding site. This quenching constant for D-mannose is consistent with the binding constant for a number of lectins [24]. It is interesting that upon denaturation of KM+ the quenching of acrylamide is significantly increased ( $K_{SV} = 5.2 \text{ M}^{-1}$ ). In the case of iodide  $K_{SV}$  increases from 0.9 to  $1.2 \text{ M}^{-1}$  suggesting the absence of cationic groups in the vicinity of tryptophan residues.

## 4. Discussion

In this paper we have demonstrated several interesting physico-chemical properties of the KM+ lectin extracted from *A. integrifolia* seeds. The CD spectrum is quite different from the CD spectra of jacalin (another lectin from *A. integrifolia*) or frutalin (a lectin from *A. incisa*, characterized by Moreira et al. [25]). It is also different from spectra normally observed for proteins with a dominant  $\beta$ -sheet structure presenting a considerable amount of unusual secondary structure (Fig. 1). The amino acid sequence of KM+ shows 52% sequence identity with jacalin [26]. Both the full amino acid sequence and the homology modelling of KM+ based on the jacalin structure, a threefold pseudo-symmetric  $\beta$ -prism structure composed of three four-stranded  $\beta$ -sheets [27], are the subject of another article [13]. Although the CD spectrum of KM+ is quite different from

that of jacalin and other  $\beta$ -proteins, nevertheless on deconvolution of this spectrum using the CCA program  $\beta$ -structure is identified as the dominant component. When the KM+ sequence is compared to that of jacalin several proline residues are observed in regions homologous to  $\beta$ -strands in the jacalin structure. It is possible that such substitutions lead to distortions in these elements of secondary structure which may perturb the CD spectrum (for example the absence of the positive peak around 200 nm) while that of jacalin is more typical of  $\beta$ -proteins. On the basis of CD data proteins have been classified into five structural classes: all- $\alpha$ , all- $\beta$  ( $\beta$ -pleated sheet),  $\alpha + \beta$  (separate regions),  $\alpha/\beta$  (intermixed regions), and random (mainly unordered) [28]. Recently, the mathematical technique of cluster analysis was proposed for the classification of a protein based on its CD spectrum [29]. Due to its non-typical CD spectrum, KM+, can not be classified into the structural classes proposed by Manavalan and Johnson [28].

The analysis of secondary structure using the CCA program showed approximately 56% of  $\beta$ -structure and 44% of random structure, normalized by removal of the contribution from others sources. The CCA program was chosen because it is a good method for deconvoluting sets of CD spectra and also because it gave a better fit to our experimental spectra (RMS 1%), as compared to the Secondary Structure Estimation program (SSE) from Jasco as well as to the Self Consistent program (SELCON) [30].

The binding constant of D-mannose to KM+ obtained by tryptophan fluorescence quenching  $(2.9 \pm 0.6) \times 10^3 \text{ M}^{-1}$  at pH 7.4, and the fraction of chromophore accessible to the quencher,  $0.43 \pm 0.08$ , showed that approximately half of the tryptophan residues in the tetramer are quenched by the sugar; it is clear that quenching of 50% of the residues is due to their proximity to the sugar binding sites, and probably the remaining 50% tryptophans are buried inside the tetramer, being inaccessible to the quenching due to the binding. These results were confirmed by KM+ primary structure, where two tryptophan residues, at positions 10 and 18, were observed. Trp18 corresponds to Trp4 in the jacalin  $\alpha$ -chain [27]. Al-

though we do not describe the homology modelling in the current article it can be inferred from such a model that Trp10 lies close to the sugar-binding pocket, while Trp18 is buried in the hydrophobic core [13].

Another interesting question is the insensitivity of KM+ to pH changes. Our CD studies suggest that the secondary structure is very stable as a function of pH showing changes only at pH 12.0, thus KM+ has a highly stable secondary structure over a large pH range. The fluorescence data show some interesting features: the fluorescence quantum yield,  $\Phi$ , has its maximal value around pH 7.0, decreasing both at acid and alkaline pH values (Fig. 5a). The decrease of  $\Phi$  at alkaline pH (twofold reduction at pH 9.0 compared to pH 7.0) suggests that some quenching mechanism is operative. Interestingly the  $\lambda_{\text{max}}^{\text{emis}}$  is constant in the pH range 4.0–9.0, increasing significantly only above pH 10.0 (Fig. 5B). This increase is consistent with an increase in solvent exposure of the tryptophan residues, due to the denatured forms at pH 12 shown in Figs. 6 and 7B, while the decrease in  $\Phi$  suggests the proximity of quencher side chains, which are in close proximity to the indol ring. At pH 12.0 quenching by  $\text{OH}^-$  can not be neglected as well.

In the present work we have reported the conformational stability of KM+ at physiological temperatures under a broad variety of conditions (urea, GdnHCl, hydrolysis, pH, etc.). It has been demonstrated that the observed changes in the tryptophan emission of KM+ are not due to multiple oligomeric species or allosteric forms of its static and excited states. An attempt was made to study the temperature-induced changes observed both in CD and fluorescence measurements. Above 328 K and around 333–338 K considerable changes are observed in the CD and fluorescence spectra, respectively. Similar properties have been reported in the literature for lectins from *Vicia villosa* (N-acetyl galactose and mannose-specific), but no thermodynamic parameters were described [31]. In the present work two types of experiments were performed in order to derive thermodynamic parameters: equilibrium experiments at a fixed incubation time and variable temperatures, and kinetic experiments at a fixed

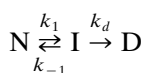
Table 1

Values of activation energy,  $E_a$ , and transition temperature,  $T_m$ , obtained with different methods

|                | CD           |              | Area of emission |              | CCA          |              |
|----------------|--------------|--------------|------------------|--------------|--------------|--------------|
|                | Equilibrium  | Kinetic      | Equilibrium      | Kinetic      | Equilibrium  | Kinetic      |
| $E_a$ (kJ/mol) | $134 \pm 11$ | $108 \pm 18$ | $179 \pm 18$     | $167 \pm 12$ | $206 \pm 18$ | $161 \pm 12$ |
| $T_m$ (K)      | $339 \pm 1$  | –            | $337 \pm 1$      | –            | $337 \pm 1$  |              |

temperature. Table 1 shows the results of the methods used to calculate the activation energy and transition temperature. It is interesting that the values obtained using both treatments of the fluorescence data are very similar. The activation energies obtained from the fluorescence measurements are greater than those from CD by 40–50% suggesting that the energetic requirements for temperature-induced changes around the tryptophan (tyrosine) residues are greater than those for the overall secondary structure.

Our results presented in this work are consistent with an irreversible thermal denaturation of KM+ ( $N \rightarrow D$ , two-state model with first order kinetics). This conclusion was arrived at from results obtained by means of different experimental approaches that covered broad temperature (298–348 K) and pH (2.2–12.0) ranges. Although the denaturation behaviour of KM+ follows a model of the type  $N \rightarrow D$  irreversible, the lack of refolding could be explained by the fact that the monomers are synthesized as precursors, and after post-translational processing, KM+ is assembled into the native tetrameric form. As a consequence, irreversible denaturation will prevent the protein refolding. This process has also been reported for jacalin, another jackfruit lectin, which binds galactose [32]. The tetrameric form, probably before reaching the denatured state is expected to dissociate producing dimers and monomers and it is interesting that these forms could not be detected for KM+ by the methods used in the present work. It is important to point out that there are other reaction schemes that can lead to first order kinetic under these conditions. The mechanism proposed by Lumry–Eyring is the following:



where I is an intermediate, which could be in our case the dissociated tetramer (free dimers and monomers), in equilibrium with the native form [33]. If it is assumed that equilibrium is always established, the formation of D will obey first order kinetics with an apparent rate constant given by:

$$k_{app} = k_d K / (K + 1) \quad (7)$$

where  $K = k_1/k_{-1}$ . When  $k_{-1} \gg k_1$  and  $k_{-1} \gg k_d$  (low temperatures), intermediate I would be present in small amounts, and remain undetected in our studies. Furthermore, K would have a value much lower than unity and  $k_{app} \cong k_d K$ . However, at higher temperature where  $k_1 \gg k_{-1}$ , the concentration of I would be expected to rise yielding as a consequence also the irreversible state D. These reaction schemes might be supported by preliminary results, in our laboratories, where the separation of the monomeric forms of KM+, with preserved secondary structure, was obtained when KM+ was eluted from reverse phase chromatography (HPLC), with organic solvents (L.M. Beltramini, unpublished data).

### Acknowledgements

The authors gratefully acknowledge Dr G.D. Fasman who provided the CCA and LINCOMB programs which have been of invaluable use to us. We thank the ‘Centro de Química de Proteínas da Faculdade de Medicina de Ribeirão Preto’ for amino acid analysis and Alexandre Marletta and Paulo S.L. Oliveira, both graduate students, for their help in the development of programs to facilitate the use of the CCA and LINCOMB

programs. We also thank Dr Richard C. Garrat for his support and critical reading of the manuscript. We acknowledge the Brazilian funding agencies CNPq, FAPESP, CAPES and FINEP for financial support.

## References

- [1] N. Sharon, H. Lis, *Science* 246 (1989) 227.
- [2] N. Sharon, *Trends Biochem. Sci.* 18 (1993) 221.
- [3] K. Drickamer, M.E. Taylor, *Annu. Rev. Cell Biol.* 9 (1993) 237.
- [4] M.P. Bevilacqua, *Annu. Rev. Immunol.* 11 (1993) 767.
- [5] S.H. Barondes, D.W. Cooper, M.A. Gitt, H. Leffer, *J. Biol. Chem.* 269 (1994) 1.
- [6] N. Sharon, H. Lis, *Sci. Am.* 268 (1993) 82.
- [7] K.A. Karlsson, *Trends Pharmacol. Sci.* 12 (1993) 265.
- [8] R.A. Moreira, J.T.A. Oliveira, *Biol. Plant.* 25 (1983) 343.
- [9] M.C. Roque-Barreira, A. Campos-Neto, *J. Immunol.* 134 (1985) 1740.
- [10] R. Santos-Oliveira, M. Dias-Baruffi, S.M.O. Thomas, L.M. Beltramini, M.C. Roque-Barreira, *J. Immunol.* 153 (1994) 1798.
- [11] P. Corbeau, M. Haran, H. Binz, C. Devaux, *Mol. Immunol.* 31 (1995) 569.
- [12] L.M. Ganiko, A.R. Martins, E.M. Espreafico, M.C. Roque-Barreira, *Glycoconjugate J.* 15 (1998) 527.
- [13] J.C. Rosa, P.S.L. Oliveira, R.C. Garrat, L.M. Beltramini, K. Resing, M.C. Roque-Barreira, L.J. Greene, *Protein Science* 8 (1999) 13.
- [14] P.S.L. Oliveira, R.C. Garrat, Y.P. Mascarenhas, L.M. Beltramini, M.C. Roque-Barreira, *Proteins Struct. Funct. Genet.* 27 (1997) 157.
- [15] A. Perczel, M. Hollósi, G. Tusnády, G.D. Fasman, *Protein Eng.* 4 (1991) 669.
- [16] A. Perczel, K. Park, G.D. Fasman, *Anal. Biochem.* 203 (1992) 83.
- [17] A. Arroyo-Reyna, A. Hernández-Arana, *Biochim. Biophys. Acta* 1248 (1995) 123.
- [18] J.M. Sánchez-Ruiz, J.L. López-Lacomba, M. Cortijo, P.L. Mateo, *Biochemistry* 27 (1988) 1648.
- [19] V.E. Yushmanov, H. Imasato, T.T. Tominaga, M. Tabak, *J. Inorg. Biochem.* 61 (1996) 233.
- [20] M.R. Eftink in: N.H. Suelter (Ed.), *Fluorescence Techniques for Studying Protein Structure, Methods of Biochemical Analysis*, vol. 35, Wiley, New York, 1991, p. 127.
- [21] E. A. Burstein, N.S. Vedenkina, M.N. Ivkova, *Photochem. Photobiol.* 18 (1973) 263.
- [22] J.R. Lakowicz, *Principles of Fluorescence Spectroscopy*, Plenum Press, New York, 1983.
- [23] M.R. Eftink, *Biophys. J.* 66 (1994) 482.
- [24] M. Rini, *Annu. Rev. Biophys. Biomol. Struct.* 24 (1995) 551.
- [25] R.A. Moreira, C.C. Castelo-Branco, A.C.O. Monteiro, R.O. Tavares, L.M. Beltramini, *Phytochemistry* 47 (1998) 1183.
- [26] N.M. Young, R.A.Z. Johnston, D.C. Watson, *FEBS Lett.* 282 (1991) 382.
- [27] R. Sankaranarayanan, K. Sekar, R. Banerjee, V. Sharma, A. Surolia, M. Vijayan, *Nat. Struct. Biol.* 3 (1996) 596.
- [28] P. Manavalan, W.C. Johnson, Jr., *Nature* 305 (1983) 831.
- [29] S.Y. Venyaminov, K.S. Vassilenko, *Anal. Biochem.* 222 (1994) 176.
- [30] N. Sreerama, R.W. Woody, *Anal. Biochem.* 209 (1993) 32.
- [31] Z.M. Shen, W.X. Shi, C. Sun, J.T. Yang, *Biochimie* 75 (1993) 949.
- [32] H. Yang, T.H. Czapla, *J. Biol. Chem.* 268 (1993) 5905.
- [33] R. Lumry, H. Eyring, *J. Phys. Chem.* 58 (1954) 110.